

Complex ion-distribution induced contrast reversal in STM imaging of DNA

Dong-Hee Kim,¹ Errez Shapir,² Hawoong Jeong,¹ Danny Porath,^{2,*} and Juyeon Yi^{3,†}

¹*Department of Physics, Korea Advanced Institute of Science and Technology, Daejeon 305-701, Korea*

²*Physical Chemistry Department, The Hebrew University, Jerusalem 91904, Israel*

³*Department of Physics, Pusan National University, Busan 609-735, Korea*

(Received 18 January 2006; revised manuscript received 22 February 2006; published 20 June 2006)

We study scanning tunneling microscope (STM) measurements of DNA molecules. It is found that the counterions along the DNA induce an attractive potential that modifies the nature of the tunneling current such that contrast inversion emerges in the STM images. By analyzing the current-distance (I - z) dependence, we demonstrate theoretically that the DNA image contrast with respect to the substrate can be reversed by changing the current setting I_{set} or the bias voltage setting V_{set} . These findings are consistent with our experimental observations of current and bias voltage dependent contrast changes in direct STM measurements.

DOI: [10.1103/PhysRevB.73.235416](https://doi.org/10.1103/PhysRevB.73.235416)

PACS number(s): 72.10.-d, 05.60.Gg, 85.65.+h, 87.15.-v

DNA is an intriguing biomolecule that has been extensively studied for decades. Recently, charge migration via the densely stacked DNA π -orbitals has attracted great attention because of its possible nanowire usage.¹ For investigating molecular properties, the scanning tunneling microscope (STM) has been used since the 1980s thanks to its high resolution and ability to provide three-dimensional data.²⁻⁶ Theoretically, most of the measurements were successfully explained by the Tersoff-Hamann (TH) orthodox theory,⁷ which gives the tunneling current, indicating the density of states and the surface topography of a given sample. The TH theory assumes that the vacuum potential is flat through the space between the STM tip and the sample. However, due to the complex ion configuration of the DNA, the vacuum potential can no longer be flat. This implies that the actual STM images of DNA molecules can be quite different from those expected within the TH picture. While other effects such as tip apex distortions can also have nontrivial effects on the resulting images, we mainly focus on the effect of the vacuum potential change on STM imaging of DNA molecules.

In this work, we evaluate the modification of the potential landscape between the tip and the molecules and examine its consequences on STM images. It is shown that the vacuum potential near the DNA molecules is strongly modified by the attractive electrostatic interactions that originate from the charge distribution on the molecules. In addition, by calculating the tunneling current via the Landauer-Büttiker formula,⁸ we find that contrast inversion (CI) can occur in STM images of DNA molecules: The relative brightness of the DNA with respect to the substrate in the images changes from darker to brighter and vice versa by controlling I_{set} or V_{set} . These contrast changes are consistent with our experimental observation of current and bias dependence of the DNA images in direct STM measurements. CI has been an unresolved problem in STM measurements.⁹⁻¹⁵ This has prompted theoretical attempts to go beyond the traditional approach. Although several studies suggested that strong interactions between the tip and the sample,¹⁶ interference between tunneling channels,¹⁷ or even tip retraction effects¹⁸ could cause image reversal, yet molecular potential effects have never been explicitly addressed until recently.¹⁹

We consider charges on the *outer* shell of the DNA, form-

ing a complex ion distribution; along the chain of the negative phosphate groups, positive ions are condensed. Let us first evaluate the effective potential from the ion distribution felt by an injected electron. The system free energy contributed from electrostatic interactions and entropy gain for spatial variance of ionic density reads,²⁰

$$\beta F = \frac{\ell_B}{2} \sum_{i,j} \frac{n_i n_j}{|x_i - x_j|} + q \ell_B \sum_i \frac{n_i}{\sqrt{x_i^2 + z^2}} + \frac{1}{2} \sum_i \frac{(n_i - n_0)^2}{(\delta n)^2} \quad (1)$$

with the Bjerrum length $\ell_B = e^2 / (\epsilon k_B T)$, q denoting the charge of the injected electron in units of e , and ϵ being the dielectric constant of the vacuum. Here x 's denote ion positions defined on a line and the perpendicular displacement from it, z , defines the position of the injected electron. The net charge (in units of e) at position x is given by $n_i = Z n_i^+ - 1$ with the mean value denoted by n_0 . Here n_i is the number density of ions of valency Z with its mean value α measuring the charge variance by $(\delta n)^2 = Z^2 \alpha$. The partition function of the system can be written as

$$\int Dn(x) \exp[-\beta F[n(x), q, z]] = Z_0 \exp[-\beta V_{\text{eff}}(q, z)].$$

After some manipulation, we obtain

$$\beta V_{\text{eff}}(q, z) = \ell_B q n_0 \frac{\sqrt{2\pi}}{a(\delta n)^2} \frac{v(0, z)}{N(0)} - \ell_B^2 q^2 \int_0^\infty dk \frac{v(-k, z)v(k, z)}{N(k) + N(-k)}, \quad (2)$$

where

$$v(k, z) = \frac{1}{\sqrt{2\pi}} \int_{-\infty}^\infty dx \frac{e^{ikx}}{\sqrt{x^2 + z^2}},$$

$$N(k) = \frac{\ell_B}{2} \int_{-\infty}^\infty dx \frac{e^{ikx}}{|x|} + \frac{1}{2a(\delta n)^2}.$$

The first term in V_{eff} depends on the net charge of the molecule n_0 ; for instance, when the molecule is neutral, this contribution vanishes. Interestingly, the second term arising

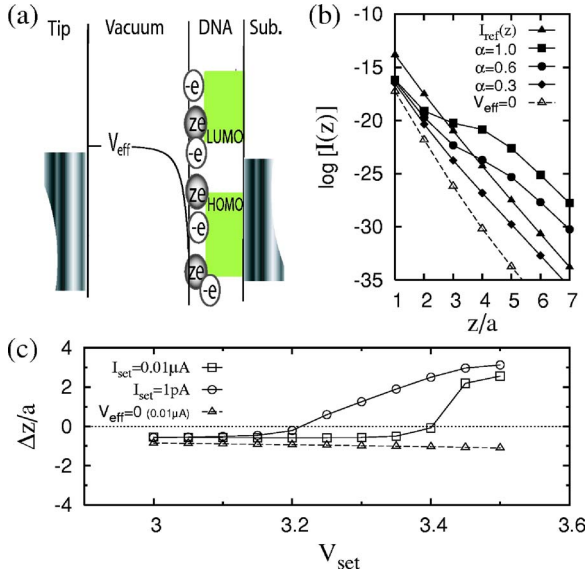


FIG. 1. (Color online) The schematic diagram of the energy configuration and the theoretically computed I - z spectroscopy in the STM measurement of DNA with monovalent counterions ($Z = 1$). (a) The effective potential is computed for $n_0 \approx -0.1$. (b) Tunneling current I as a function of tip-sample distance z for various counterion concentrations α at $V_{\text{set}} = 3.35$ V. The tip-substrate current in the absence of DNA samples (I_{ref}) is drawn in the same plot. (c) V_{set} dependence of Δz at the current sets, $I_{\text{set}} = 0.01 \mu\text{A}$ and 1 pA for $\alpha = 1$. In (b) and (c), the results disregarding the DNA effective potential ($V_{\text{eff}} = 0$) are shown for comparison.

from charge variance is always negative, irrespective of n_0 . This attraction dominates, so that even if the molecule is negatively charged, the effective potential becomes attractive [see Fig. 1(a)]. It is important that it lowers the tunneling barrier between the tip and the DNA, given by the work function. As shown in Fig. 1(a), the effective potential induces a potential dip near the DNA. For instance, for $Z = 1$ and $\alpha = 1.0$, the potential dip is located at ~ 1.7 eV below the work function value, and the dip gets back to the work function value as α decreases.

The presence of the electrostatic potential due to the ion complex distribution as seen in Eq. (2) transforms the vacuum level from flat into structured. To investigate the electrostatic potential effect on the tunneling current, we adopt the Landauer-Büttiker formula,⁸ which gives the current from the tip to the substrate through the DNA sample at a voltage bias V :

$$I(V) = \frac{2e}{h} \int_{-\infty}^{\infty} dE T(E) [f_t(E + eV) - f_s(E)], \quad (3)$$

where $f_{t,s}(E) = (\exp[(E - \mu_{t,s})/kT] + 1)^{-1}$ are the distribution functions of electrons at the tip and the substrate, respectively. We assume that the Fermi level is $\mu_{t,s} = 0.0$ eV. A nonequilibrium Green function formalism²¹ is used to obtain the transmission $T(E)$ through the system,

$$T(E) = \text{tr}(\Gamma_t G^r \Gamma_s G^{r\dagger}) \quad (4)$$

with the retarded Green function $G^r = (E + i0^+ - H - \Sigma_t - \Sigma_s)^{-1}$. The self-energy contribution is made by coupling the mol-

ecule to the tip and to the substrate, leading to coupling matrices as $\Gamma_{t,s} = -2 \text{Im} \Sigma_{t,s}$. The molecule Hamiltonian is composed as

$$H = H_v + H_{\text{DNA}} + H_c, \quad (5)$$

where H_v describes the electron motion in vacuum as

$$H_v = \sum_{i=0}^n [\varepsilon_i c_i^\dagger c_i - t_v (c_i^\dagger c_{i+1} + \text{H.c.})],$$

with $\varepsilon_i \equiv W + V_{\text{eff}}(z_i) + 2t_v$ and $t_v \equiv \hbar^2 / (2ma^2)$. H_v is written in the discrete form by applying the finite difference method to the single-particle Hamiltonian,²² where we discretize the space in units of a as $z_i = a(i+1)$ that with $i=n$ determines the tip height denoted by z hereafter. The unit length is chosen as $a = 3 \text{ \AA}$, a little less than the inter-base spacing in a strand (any finer length scale would not alter the physics presented here but cost more for the numerical evaluation). For electronic conduction through a poly(G)-poly(C) molecule, H_{DNA} was proposed as²³

$$H_{\text{DNA}} = \sum_{\alpha=G,C} \sum_i U_\alpha(i) d_{\alpha i}^\dagger d_{\alpha i} - t_\alpha (d_{\alpha i}^\dagger d_{\alpha i+1} + \text{H.c.}),$$

where the on-site potential is given by $U_G(i) = (-1)^i U_G$ and $U_C(i) = (-1)^{i+1} U_C$. This potential, alternating over bases, originates from charge-density-wave formation due to strong Coulomb repulsion between bases. This empirical Hamiltonian is shown to yield current-voltage characteristics in good accordance with experimental results. We use the parameter set: $U_G = U_C = 0.8$ eV, $t_C = 0.3$ eV, $t_G = 0.2$ eV that properly describes the conduction characteristics of DNA molecules.²³ We also have the Hamiltonian connecting the vacuum and DNA sector as

$$H_c = -t_{vd} (c_0 d_{G0}^\dagger + c_0 d_{C0}^\dagger + \text{H.c.}),$$

where $d_{\alpha 0}^\dagger$ represent particle creation operator at a base closest to the tip, and t_{vd} remains as an adjustable parameter for changing the current offset. Finally, the self-energy contribution due to the system-leads (tip and substrate) coupling can be written as $\Sigma_t = (\gamma_t/2i) c_n^\dagger c_n$ and $\Sigma_s = (\gamma_s/2i) \sum_\alpha \sum_i d_{\alpha i}^\dagger d_{\alpha i}$.²⁴

Now suppose a STM measurement of a DNA molecule in constant-current mode where the vertical tip position z is adjusted to retain the tunneling current $I(z) = I_{\text{set}}$ with fixed V_{set} . The I - z characteristic directly indicates the contrast (relative brightness) of the DNA sample with respect to the substrate. Assume that the tunneling current to the substrate is given by $I_{\text{ref}}(z)$ and $I(z)$ in the absence and in the presence of a DNA molecule, respectively. When the tip is over a DNA-free region, the tip position z_{ref} is obtained by $I_{\text{ref}}(z_{\text{ref}}) = I_{\text{set}}$; moving the tip horizontally to a position above the DNA molecule, z_{ref} is changed into z_{DNA} satisfying $I(z_{\text{DNA}}) = I_{\text{set}}$. This tip displacement $\Delta z = z_{\text{DNA}} - z_{\text{ref}}$ is translated into the contrast: Positive (negative) z indicate brighter (darker) image of the molecule.

The I - z characteristics are calculated by Eqs. (3) and (4) with the elements introduced above for various configurations of DNA molecules [see Fig. 1(b)]. While $I_{\text{ref}}(z)$ clearly shows the exponential decaying behavior expected from the

TH theory, $I(z)$ turns to nonlinear and crosses the reference line at $I(z_c) = I_{\text{ref}}(z_c) \equiv I_c$. This deviation comes from the presence of an effective potential between the tip and the ion complex distribution. When we turn off the potential ($V_{\text{eff}} = 0$), the current decaying behavior goes back to the exponential decay with the reduced amplitude due to the relatively poor conductivity of DNA molecules.

This nonexponential crossover behavior of the tunneling current has an interesting consequence on STM images of DNA: The contrast of the DNA images can be reversed by changing I_{set} . When I_{set} is set to be higher than I_c , we read off a smaller tip height above the molecule than above the substrate by following the I - z characteristics [see Fig. 1(b)]: The sample is imaged as an indentation ($\Delta z < 0$, darker than the substrate). On the other hand, when lowering I_{set} below I_c , the tip height above the molecule becomes larger than that above the substrate: A protruded image of the DNA ($\Delta z > 0$, brighter image) appears.

The described CI phenomenon depends on α , the number density of ions. If α is too small to allow the crossover behavior of $I(z) = I_{\text{ref}}(z)$, then no image reversal can be observed. This theoretical prediction indirectly suggests that image reversal can happen even without changing I_{set} , that is, *spontaneous* CI. Assume that the ionic configuration of the molecule undergoes a large spatial change in α . Then, for example, at $I_{\text{set}} = 1$ pA, while the scan shows a brighter image when the tip is above a domain with $\alpha = 1$, the contrast would be inverted to darker when the tip scans a molecule domain with $\alpha = 0.3$ [see Fig. 1(b)].

CI can be also obtained by changing V_{set} instead of I_{set} . The sign change of Δz at a certain bias voltage V_c , where $\Delta z(V_c) = 0$, indicates the indentation-protrusion transition of the DNA image. The DNA molecule is seen as an indentation ($\Delta z < 0$), for $V_{\text{set}} < V_c$. When increasing V_{set} above V_c , the molecule becomes a protrusion ($\Delta z > 0$). For comparison, we present Δz when neglecting V_{eff} , in which the molecule should always be imaged darker than the substrate.

The above features are demonstrated by our STM measurements on poly(dG)-poly(dC), λ -DNA and G4-DNA molecules.^{19,25,26} We addressed an experimental layout of DNA molecules, 4000 base pairs long, deposited from a solution of tris acetate (pH=7.0) onto a highly smoothed gold (111) surface achieved by a flame annealing process. The immobilization of the molecules on the substrate is crucial, since DNA molecules are commonly displaced by the STM tip during scanning. Here, we used an electrostatic deposition method, in which the gold surface was positively biased (0.18 V with respect to a counter electrode in the solution) during the incubation of the DNA solution on the substrate, or chemical adsorption using a thiol group on one end of each molecule. All the presented measurements were performed at room temperature (RT) and at $T \sim 78$ K at ultra-high vacuum conditions ($\sim 5 \times 10^{-11}$ mbar) with a commercial Omicron LTSTM system using chemically etched tungsten tips. Full details of the DNA characterization and STM imaging appear in Ref. 26.

CIs induced by changing I_{set} are shown in Fig. 2, which demonstrates three consecutive STM scans of DNA molecules measured in constant current mode at $V_{\text{set}} \sim 2.8$ V. In

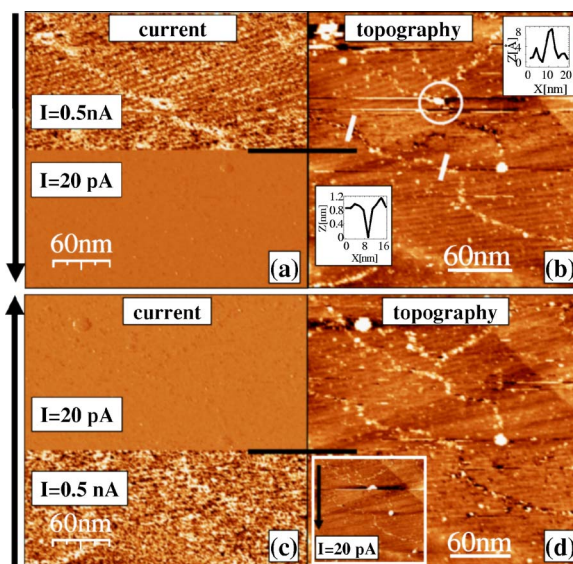


FIG. 2. (Color online) Demonstration of current-controlled CI in DNA STM images. Downward [(a),(b)] and upward [(c),(d)] scans, performed on the same area, are presented by current [(a),(c)] and topography [(b),(d)] maps. In both scans, the initial I_{set} , 0.5 nA, is changed to 20 pA at the black lines followed by an inversion of the DNA image contrast from negative to positive. Similar CI is observed from scan (b) to (d) when changing I_{set} from 20 pA to 0.5 nA. The insets in (b) show the tip heights along the white marks in negative and positive contrast domains of the molecule. Note the spontaneous inversion observed in (b) (white circle). The inset in (d) is rescanned with fixed $I_{\text{set}} = 20$ pA after the previous scans and shows that the molecule is physically intact.

these scans, I_{set} is changed during the scanning while other scan parameters are fixed. The topography maps [Figs. 2(b) and 2(d)] demonstrate controlled inversions of the DNA image contrast (bright represents “high” and dark represents “low”) upon changing I_{set} : The DNA appears dark at $I_{\text{set}} = 0.5$ nA and changes to bright when changing I_{set} to 20 pA and vice versa. The corresponding current maps [Figs. 2(a) and 2(c)] emphasize visually the two current zones (high current—bright, low current—dim) of the scanned areas.

Spontaneous CIs are observed as well.¹⁹ While a scan of a certain domain of the molecule gives a bright image, a different domain of the same molecule appears dark although no changes in I_{set} took place [see the white circle in Fig. 2(b)]. Such spontaneous CI may have a few origins. A sudden change in the tip apex shape may induce CI by invoking an irregular potential landscape between the tip and the molecule. A more theoretical explanation for the CI is, as stated above, based on the spatial variation of α . Accidental tip contamination is, on the other hand, unlikely since the consecutive scan confirms that a molecule is physically intact [see the inset in Fig. 2(d)], which is also supported by the fact that the gold substrate appears clean and with details usually observed with a clean tip only.

Figure 3 demonstrates the effect of V_{set} on the contrast of the DNA images in constant current mode. In Fig. 3(a), V_{set} is changed during the scan from 2.5 to 1 V with fixed I_{set} . The full height of the DNA, ~ 1 nm, is revealed in the upper part of the image, scanned with $V_{\text{set}} = 2.5$ V, while at the

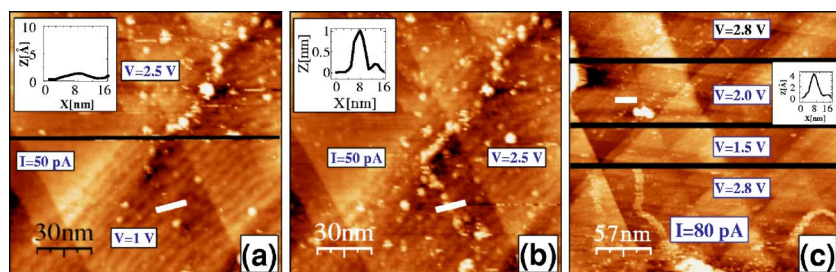


FIG. 3. (Color online) Bias-dependent STM images measured in constant current mode with $I_{\text{set}}=50$ pA at room temperature (a), (b) and $I_{\text{set}}=80$ pA at 78 K (c). The nearly transparent part of the molecule at $V_{\text{set}}=1$ V [(a)—lower part] is changed into clearly protruding from the substrate in the following scan, (b), at $V_{\text{set}}=2.5$ V. The insets in (a) and (b) compare the tip heights along the white marks at the same spot on the molecule, where the 7 Å height difference is evident. Consecutive V_{set} changes in (c) show a more detailed V_{set} -dependence of the image contrast. Note that when V_{set} is returned to 2.8 V, the molecule apparent height is restored.

lower part of the image, scanned at $V_{\text{set}}=1$ V, the molecules are almost transparent. The whole subsequent scan, measured at 2.5 V, shows the full height of the DNA in the same area where it appeared nearly transparent in the previous scan. The tip height measurements are taken at the same spot (white lines) on the DNA in both scans, showing a clear tip height change from ~ 2 Å ($V_{\text{set}}=1$ V) to ~ 9 Å ($V_{\text{set}}=2.5$ V) [see Figs. 2(a) and 2(b)].

A more detailed measurement of V_{set} -dependent contrast variation is obtained by subsequent voltage changes in a single scan [see Fig. 3(c)]. The measurement shows apparent DNA height changes upon gradual voltage changes. Initially, when V_{set} is 2.8 V, a maximum height, ~ 8 Å, is achieved (brightest contrast); at $V_{\text{set}}=2$ V the contrast decreases to ~ 4 Å and at $V_{\text{set}}=1.5$ V, the molecule becomes transparent. Upon returning V_{set} to 2.8 V, the apparent molecule height is restored. Although full inversion is not observed here, the contrast change is clear. Throughout the entire scan, the image of the underlying gold surface is unchanged and the DNA molecule remains intact, as seen in scans before and after those shown in Fig. 3(c), suggesting that the contrast changing behavior is a pure electrical effect.

CI in STM imaging of molecules is an intricate phenom-

enon, depending also on uncontrolled parameters, e.g., the strengths of the charge variance, the tip-sample coupling, the effect of the tip shape, and so on. It is not plausible to incorporate all those effects explicitly in the theory that, hence, cannot provide full details of the experimental observations. For instance, the theoretically predicted value of the voltage for the CI onset is higher than the observed value. This implies that the actual charge variance along the molecules might be more severe than accounted for by the Gaussian theory. Nevertheless, our theoretical model provides a reasonable explanation to many aspects of the experimental observations, and salient picture for a better understanding of STM images of DNA molecules.

We thank Gianarelio Cuniberti and Igor Brodsky for fruitful discussions and H.J. would like to thank KIAS for the support during the visit. The research was supported by the FIRST Foundation, The Israeli Academy of Sciences and Humanities, The German Israel Foundation, European grant for Future & Emerging Technologies (IST-2001-38951), Korea Research Foundation (KRF-2004-005-C00044), and Korean Science and Engineering Foundation (R04-2004-000-10031).

*Email address: porath@chem.ch.huji.ac.il

†Email address: jyi@pusan.ac.kr

- ¹D. Porath, G. Cuniberti, and R. Di Felice, *Top. Curr. Chem.* **237**, 183 (2004); C. Dekker and M. A. Ratner, *Phys. World* **14**, 29 (2001); R. G. Endres, D. L. Cox, and R. R. P. Singh, *Rev. Mod. Phys.* **76**, 195 (2004); M. D. Ventra and M. Zwolak, in *Encyclopedia of Nanoscience and Nanotechnology*, edited by H. S. Nalwa (American Scientific, CA, 2004); D. Porath, D. N. Lapidot, and J. Gomez-Herrero, in *Lecture Notes in Physics Series*, edited by G. Cuniberti, G. Fagas, and K. Richter (Springer, Berlin, 2005); Rafael Gutierrez, Danny Porath, and Gianarelio Cuniberti, in *Charge Transport in Disordered Solids with Applications in Electronics*, edited by Sergey Baranovski (Wiley, New York, 2006), ISBN: 0-470-09504-0.
- ²T. P. Beebe, T. E. Wilson, D. F. Ogletree, J. E. Katz, R. Balhorn, M. Salmeron, and W. Siekhaus, *Science* **243**, 370 (1989); R. J.

Driscoll, M. G. Youngquist, and J. D. Baldeschwieler, *Nature (London)* **346**, 294 (1990).

- ³E. L. Wolf, *Principles of Electron Tunneling Spectroscopy* (Oxford Science, London, 1989).
- ⁴M. G. Youngquist, R. J. Driscoll, T. R. Coley, W. A. Goddard, and J. D. Baldeschwieler, *J. Vac. Sci. Technol. B* **9**, 1304 (1991).
- ⁵S. M. Lindsay, Y. L. Lyubchenko, N. J. Tao, Y. Q. Li, P. I. Oden, and J. A. DeRose, *J. Vac. Sci. Technol. A* **11**, 808 (1993).
- ⁶T. E. Wilson, M. N. Murray, D. F. Ogletree, M. D. Bednarski, C. R. Cantor, and M. B. Salmeron, *J. Vac. Sci. Technol. B* **9**, 1171 (1991).
- ⁷J. Tersoff and D. R. Hamann, *Phys. Rev. B* **31**, 805 (1985).
- ⁸M. Büttiker, Y. Imry, R. Landauer, and S. Pinhas, *Phys. Rev. B* **31**, 6207 (1985).
- ⁹A. R. H. Clarke, J. B. Pethica, J. A. Nieminen, F. Besenbacher, E. Lægsgaard, and I. Stensgaard, *Phys. Rev. Lett.* **76**, 1276 (1996).

- ¹⁰D. P. Allison, L. A. Bottomley, T. Thundat, G. M. Brown, R. P. Woychik, J. J. Schrick, K. B. Jacobson, and R. J. Warmack, *Proc. Natl. Acad. Sci. U.S.A.* **89**, 10129 (1992).
- ¹¹S. M. Lindsay and B. J. Barris, *J. Vac. Sci. Technol. A* **6**, 544 (1988).
- ¹²T. Thundat, L. A. Nagahara, P. Oden, and S. M. Lindsay, *J. Vac. Sci. Technol. A* **8**, 645 (1990).
- ¹³L. A. Bottomley and J. N. Haseltine, *J. Vac. Sci. Technol. A* **10**, 591 (1992).
- ¹⁴D. P. Allison, T. Thundat, K. B. Jacobson, L. A. Bottomley, and R. J. Warmack, *J. Vac. Sci. Technol. A* **11**, 816 (1993).
- ¹⁵T. Kawai, H. Tanaka, and T. Nakagawa, *Surf. Sci.* **386**, 124 (1997).
- ¹⁶G. Doyen, D. Drakova, and M. Scheffler, *Phys. Rev. B* **47**, 9778 (1993); H. Ness and A. J. Fisher, *ibid.* **55**, 10081 (1997).
- ¹⁷J. Nieminen, S. Lahti, S. Paavilainen, and K. Morgenstern, *Phys. Rev. B* **66**, 165421 (2002).
- ¹⁸S. M. Lindsay, T. Thundat, and L. Nagahara, *J. Microsc.* **152**, 213 (1988).
- ¹⁹E. Shapir, J. Yi, H. Cohen, A. B. Kotlyar, G. Cuniberti, and D. Porath, *J. Phys. Chem. B* **109**, 14270 (2005).
- ²⁰A. W. C. Lau and P. Pincus, *Phys. Rev. Lett.* **81**, 1338 (1998); B.-Y. Ha and A. J. Liu, *ibid.* **79**, 1289 (1997); R. Golestanian, M. Kardar, and T. B. Liverpool, *ibid.* **82**, 4456 (1999).
- ²¹Y. Meir and N. S. Wingreen, *Phys. Rev. Lett.* **68**, 2512 (1992).
- ²²S. Datta, *Electronic Transport in Mesoscopic Systems* (Cambridge University Press, New York, 1995).
- ²³J. Yi, *Phys. Rev. B* **68**, 193103 (2003).
- ²⁴Wide-band leads are considered so that the self-energy and thereby the coupling are regarded as energy-independent.
- ²⁵A. B. Kotlyar, N. Borovok, T. Molotsky, H. Cohen, E. Shapir, and D. Porath, *Adv. Math.* **17**, 1901 (2005).
- ²⁶E. Shapir, H. Cohen, N. Borovok, A. B. Kotlyar, and D. Porath, *J. Phys. Chem. B* **131**, 367 (2006).